ENVIRONMENTAL STUDIES

The gathering firestorm in southern Amazonia

P. M. Brando[1,2,3]*, B. Soares-Filho[4], L. Rodrigues[4], A. Assunção[4], D. Morton[5], D. Tuchschneider[6], E. C. M. Fernandes[6], M. N. Macedo[2,3], U. Oliveira[4], M. T. Coe[2,3]

Wildfires, exacerbated by extreme weather events and land use, threaten to change the Amazon from a net carbon sink to a net carbon source. Here, we develop and apply a coupled ecosystem-fire model to quantify how greenhouse gas–driven drying and warming would affect wildfires and associated CO_2 emissions in the southern Brazilian Amazon. Regional climate projections suggest that Amazon fire regimes will intensify under both low- and high-emission scenarios. Our results indicate that projected climatic changes will double the area burned by wildfires, affecting up to 16% of the region's forests by 2050. Although these fires could emit as much as 17.0 Pg of CO_2 equivalent to the atmosphere, avoiding new deforestation could cut total net fire emissions in half and help prevent fires from escaping into protected areas and indigenous lands. Aggressive efforts to eliminate ignition sources and suppress wildfires will be critical to conserve southern Amazon forests.

INTRODUCTION

Greenhouse gas (GHG) emissions accumulating in the atmosphere may push Amazon forests into a new low-biomass state by altering regional precipitation and temperature regimes. This climate-induced forest transition has the potential to release large amounts of GHGs to the atmosphere and accelerate global warming (*1*). Although CO_2 fertilization of forests may partially offset this forest dieback (*2*), most models lack representation of important negative processes such as wildfires (*3*). Fire disturbance is already driving large-scale forest mortality across the drier portions of the Amazon basin (*4*) and is likely to expand into wetter areas as climate and land use change (*5*). Ignoring this potentially large source of GHG emissions to the atmosphere may restrict our ability to mitigate climate change and, consequently, undermine effective conservation of Amazon forests. Better understanding of future fire regimes in Amazonia could help guide efforts to increase regional capacity to prevent accidental forest fires and their negative impacts on ecosystem services, socioeconomic well-being, and biodiversity (*6*).

Deforestation in the Brazilian Amazon declined by 70% between 2004 and 2014 (*7*), avoiding the equivalent of 12% of global annual CO_2 emissions (*8*), the main GHG causing climate change. Over the same period, emissions of CO_2 and other GHGs associated with wildfires (e.g., CO, CH_4, NO_x, and N_2O) accelerated. Interactions between agricultural activities, illegal fires, and extreme weather events intensified Amazon fire regimes and their associated emissions (*9*, *10*). During the 2000s alone, ~85,000 km^2 of primary forests burned in Amazonia, mostly during the 2005 and 2010 droughts linked to the warm phase of the Atlantic Multidecadal Oscillation (AMO) (*9*). In 2015, the central Amazon experienced a similar spike in fire activity during another severe and widespread drought event, triggered by anomalous warming of both the tropical Pacific (El Niño) and the tropical North Atlantic (*9*). Superimposed upon these episodic droughts, climate change will likely promote even more frequent, intense, and extensive drought events. The strong climatic control over these wildfire events (*11*) suggests that forest flammability will increase in the near future, especially if deforestation rates increase but even if they decline (*5*). Addressing large-scale forest degradation by Amazon wildfires is therefore critical to quantifying future global GHG emissions.

In Amazonia, surface forest wildfires emit GHGs to the atmosphere via three main mechanisms. First, the combustion of fuels (e.g., leaves, twigs, and branches) instantly transfers CO_2 to the atmosphere, with most tropical wildfires contributing between 20 and 60 MgC ha^{-1} (*12*–*14*). Second, thermal degradation of biomass causes the release of several types of GHGs other than CO_2, including methane (CH_4), nitrous oxide (N_2O), carbon monoxide (CO), and nitrogen oxides (NO_x). Last, post-fire tree mortality contributes CO_2 emissions to the atmosphere for several years or decades as trees continue to die and decompose (*13*–*15*). Although forest recovery can offset CO_2 emissions associated with post-fire tree mortality, recovery may be slowed when high-intensity fires kill seeds and bud (resprout) banks and create niche spaces for invasive species such as grasses (*14*).

Here, we used a coupled fire-ecosystem model (fig. S1) to assess the synergies between climate change and deforestation in determining burned area (BA) and fire-induced emissions of CO_2, CO, CH_4, N_2O, and NO_x (hereafter referred to as eCO_2) from the driest portions of the Amazon. This region represents 61% of the Brazilian Legal Amazon (Fig. 1) and is a hot spot of forest fire activity (*10*). Our fire model simulates daily fire ignition and spread as a function of climatic conditions, land use, fuel loads, and terrain at 500-m resolution. Our ecosystem model also represents forest carbon (C) dynamics and drought-induced changes in fuel loads and drying—a process that is absent in most ecosystem models (fig. S1). We used this coupled model to test the hypothesis that future forest fires will be highest where (i) forest edges are exposed to ignition sources due to deforestation and fragmentation and (ii) climate becomes drier and hotter because of the accumulation of atmospheric GHGs. Conversely, BA could decrease where high deforestation reduces forest connectivity and associated fuel continuity, despite the presence of flammable edges. We also expected low BA where dense primary forests create a moist understory microclimate (*16*). The latter includes the interior of protected areas and indigenous reserves, referred to here as protected

[1]Department of Earth System, University of California, Irvine, CA 92697, USA. [2]Woods Hole Research Center, 149 Woods Hole Rd., Falmouth, MA 02540, USA. [3]Instituto de Pesquisa Ambiental da Amazônia (IPAM), SHIN, CA-5, Brasilia, DF 7500, Brazil. [4]Centro de Sensoriamento Remoto, Instituto de Geociências, Universidade Federal de Minas Gerais (UFMG), Av. Antônio Carlos 6627, CEP 31270-901, Belo Horizonte, MG, Brazil. [5]NASA Goddard Space Flight Center, Greenbelt, MD 20771, USA. [6]Agriculture Global Practice, World Bank Group, 1818 H. St., NW, Washington, DC 20433, USA.
*Corresponding author. Email: pbrando@uci.edu

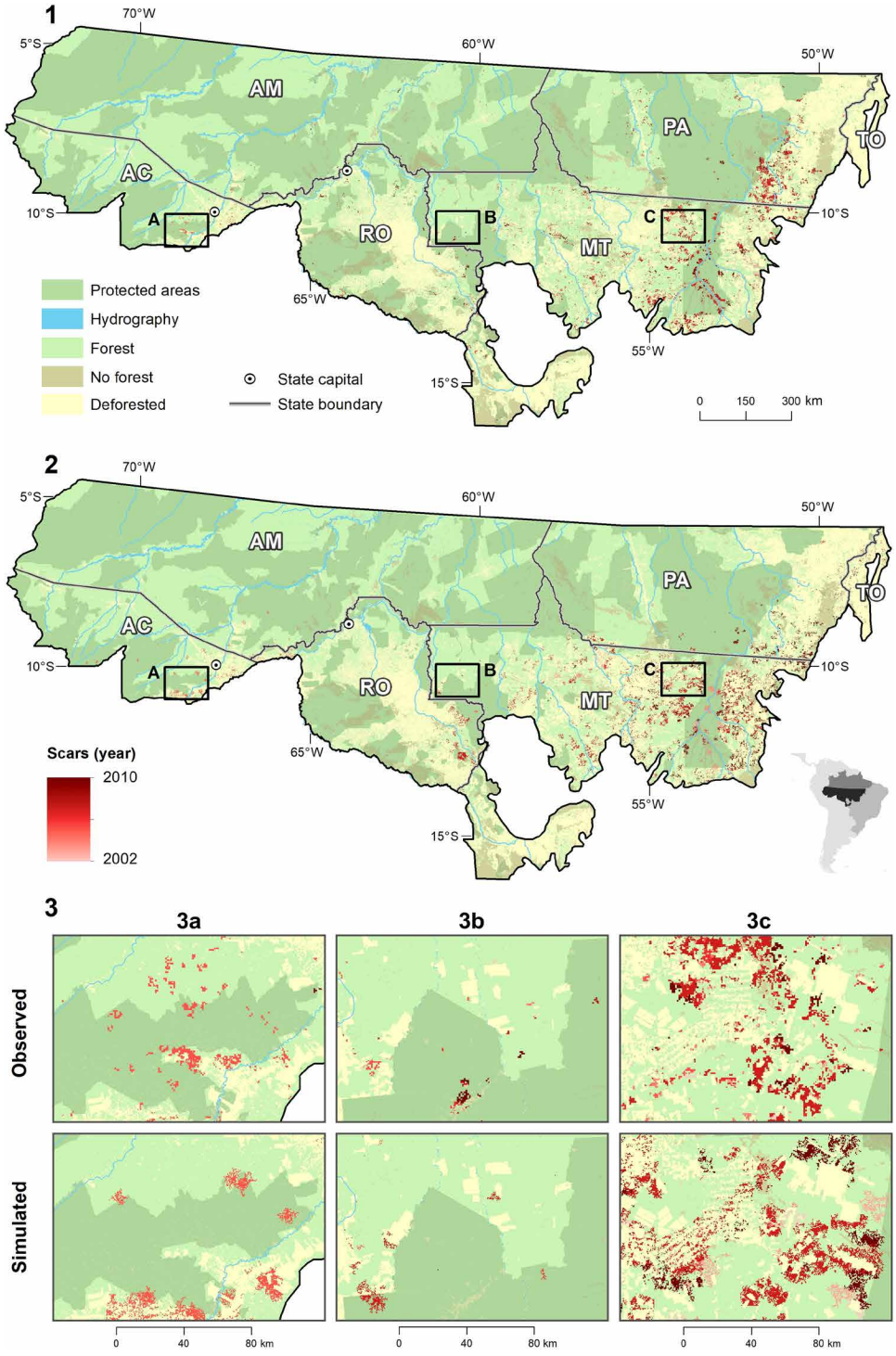

Fig. 1. Historical patterns of BA across Brazil's southern Amazon for the period 2002–2010. 1 (top): Observed fire scars from Morton *et al.* (*10*). **2** (middle): Simulated fire scars based on our fire model [fire ignition and spread for C (FISC)]. **3** (bottom): Observed (upper panels) and simulated (lower panels) patterns of BA for three regions of the southern Amazon (indicated on the upper panels).

forests. Our model simulations from 2000 to 2050 represent two scenarios of climate change [low emissions: representative concentration pathway 2.6 (RCP2.6); high emissions: RCP8.5], two scenarios of deforestation [following recent trends (D) and no deforestation (N)], and their combination (RCP2.6D, RCP 8.5D, RCP2.6N, and RCP 8.5N).

RESULTS

Model robustness

Our probabilistic fire model captured broad spatial and temporal patterns of ignition sources and BA for the southern Brazilian Amazon (Fig. 1). The simulated number of hot pixels (our proxy for fire ignitions)

was highest during the dry season and lowest during the wet season (Fig. 2), when low vapor pressure deficit (VPD) usually damps forest flammability to zero (*16*). The simulated number of hot pixels approximated observed patterns [R^2: 0.83; slope: 1.60; root mean square error (RMSE): 2431.88; Fig. 2], although there were fewer simulated ignition sources than observed. Simulated regional and temporal patterns of fire scars also agreed with observations (R^2: 0.88; slope: 0.88; RMSE: 0.18) (Fig. 2). Specifically, the BA peaked during dry, hot years and occurred mostly along forest edges across the Arc of Deforestation, consistent with BA patterns typical of the southern Amazon in recent decades (*10*, *11*).

In addition to capturing spatial and temporal patterns of BA, our modeling framework properly represented observed patterns of fire intensity and severity in southern Amazonia. Once a given forested pixel ignited, our ecosystem model simulated the fireline intensity from fuel consumption (*W*), fire spread rate (FSR), and the constant heat yield per unit of fuel combusted. Compared with observed values from a large-scale fire experiment in southeast Amazonia (*4*), the modeled fireline intensity and associated variables (*W* and FSR) performed relatively well during drought and nondrought years (Fig. 3). Fire intensity during the droughts of 2007 and 2010 was substantially higher than that during the nondrought years because of the simulated variability in understory VPD and fuel availability. On the other hand, our model overestimated FSR by 48%, underestimated fuel consumption by 25% during nondrought years, and overestimated fuel consumption by 18% during drought years. This suggests that the simulated fires could lead to higher mortality.

Our coupled fire-ecosystem model was most sensitive to variability in understory VPD, with drought [as represented by the maximum climatological water deficit (MCWD)] having an important secondary effect (fig. S2). Thus, BA and eCO_2 emissions from wildfires occurred mostly during drought years that caused canopy opening and increased understory VPD.

Fire regimes in a changing climate—No new deforestation

Even with no new deforestation, simulated fire regimes intensified across the southeast Amazon under climate change scenarios RCP8.5N and RCP2.6N. Compared to the 2000s, simulated forest fires in subsequent decades burned larger areas, combusted more fuels, released more energy, and emitted more eCO_2 to the atmosphere (Fig. 4). Gross emissions of eCO_2 from these fires totaled 16.5 Pg (RCP 2.6N) and 13.7 Pg (RCP8.5N) by 2050. For the period 2001–2050, the RCP8.5N

Fig. 2. Seasonal patterns of active fires in deforested areas near forest edges (≤4 km) for the southern Amazon. (**A**) Seasonal patterns in active fires ("hot pixels") in deforested areas near forest edges for the southern Amazon in 2003. "Observed" stands for NOAA—12 satellite night active fires (*10*), while "Simulated" stands for FISC active fires. The correlation between observed and simulated active fires was strong ($r^2 = 0.91$) and significant ($P < 0.01$). (**B**) Annual variability in BA (understory fires) for the southern Amazon using a coupled fire-ecosystem model. The correlation between observed (*10*) and simulated active fires was strong ($r^2 = 0.94$) and significant ($P < 0.01$).

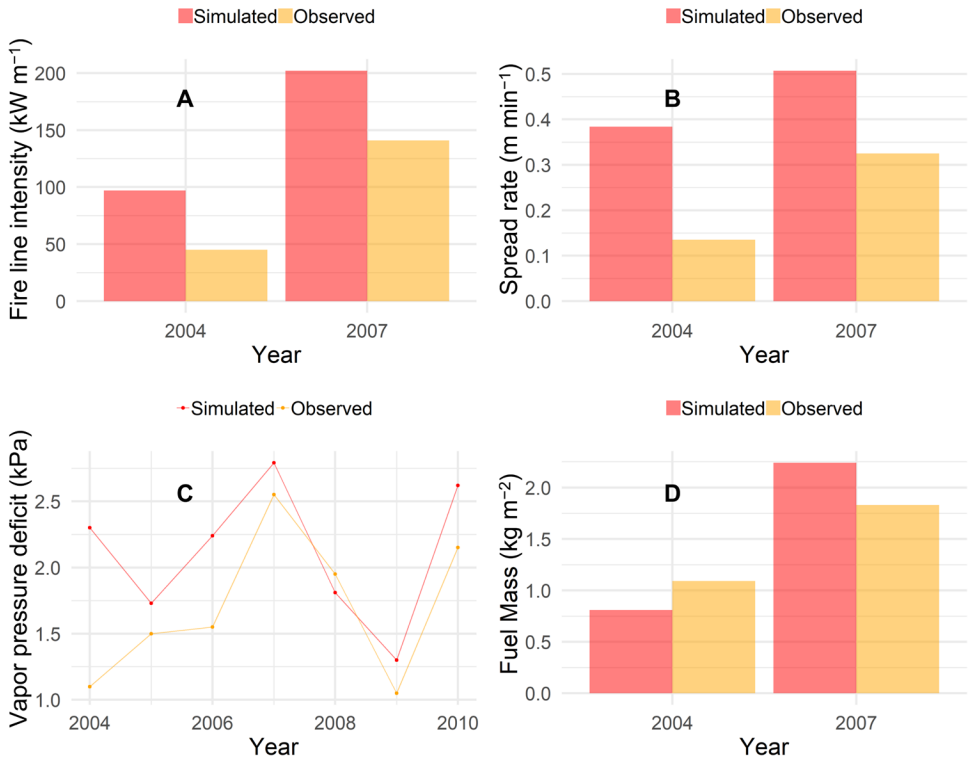

Fig. 3. Simulated and observed patterns in fire behavior for southeast Amazonia. Observed data were collected in the context of a large-scale fire experiment, in which 50-ha experimental plots were burned annually (with the exception of 2008) or triennially between 2004 and 2010 (*6*). During 2007 and 2010, the region experienced severe droughts and increased air temperature. (**A**) Fireline intensity. (**B**) Rate of fire spread. (**C**) Understory VPD. (**D**) Fuel mass consumed by the experimental fires.

scenario resulted in more severe fires but reduced BA, compared to the conservative GHG emission scenario (RCP2.6N). As a result, the model projected higher gross GHG emissions in RCP2.6N than in RCP8.5N for the entire period. After the 2030s, BA and eCO_2 increased more in RCP8.5N than in RCP2.6N, suggesting that the radiative forcing of 8.5 W had increasingly important effects on fire regimes as climatic conditions changed (table S1).

Fire regimes in a changing climate—BAU deforestation

When we accounted for new deforestation in our simulations, BA and fire-related eCO_2 emissions increased under both climate scenarios (RCP8.5D and RCP2.6D), compared to the no-deforestation simulations (RCP8.5N and RCP2.6N). Under RCP8.5D, simulated BA and gross eCO_2 emissions from forest fires totaled 22.3 Mha and 17.0 Pg, respectively, between 2010 and 2050. These values were 30 and 22% higher than in RCP8.5N (Fig. 4), suggesting strong interactions between climate change and deforestation in the near future. Overall, the scenario representing deforestation and high radiative forcing (RCP8.5D) yielded the highest gross eCO_2 emissions from wildfires. In contrast, climate scenarios without new deforestation yielded the lowest fire-related eCO_2 emissions (tables S1 and S2).

As deforestation interacted with climate change in our simulations, the number and geography of Amazon wildfires changed compared to current BA (Fig. 5). A 5% decline in forest area from 2010 to 2050 (due to deforestation) increased the simulated BA by 47% (RCP8.5D) and 40% (RCP2.6D) (Fig. 4). In the scenario representing business-as-usual (BAU) deforestation rates, drought-induced fuel accumulation and drying increased wildfire activity, even in areas experiencing low deforestation. Although protected areas and indigenous lands effectively deterred most deforestation, these forests experienced an actual increase in BA in the future (from 27 to 42%) due to the combined effects of high fuel loads, increased dryness, and fuel continuity. In older frontiers with more fragmented forests, the projected BA decreases (from 73 to 58%), probably because of the lack of large forest blocks available to burn. In addition, BA was already extremely high in the beginning of our simulations, so there was little room to further increase.

Post-fire recovery—Net emissions

Most fire-related GHG emissions in our simulations resulted from combustion and post-fire tree mortality releasing CO_2 to the atmosphere. CO_2 and CO accounted for 70 and 7% of total emissions, respectively. Together, other GHGs contributed 23% (table S1). Although we expected post-fire forest regrowth to partially offset CO_2 emissions, our simulations show lower capacity of forests to recover their C stocks in the near future. Future dry-warm climatic conditions caused reduced C stocks due to high-severity fires and larger BA. Post-fire recovery of C stocks also decreased because future climate conditions reduce potential forest biomass. As a result, we project that a greater proportion of C emissions from future forest fires will remain in the atmosphere rather than being assimilated back into forests. Assuming average rates of biomass recovery, cumulative net C emissions (emissions minus recovery) from these fires could reach 1 PgC for both RCP2.6N and RCP8.5D scenarios between 2010 and 2050. However, our simulations show that avoiding new deforestation could reduce net emissions by 38% (RCP2.6) and 56% (RCP8.5D). Preventing repeated burning could also promote faster forest recovery of C stocks, given that 26% of the study region experienced repeated burning.

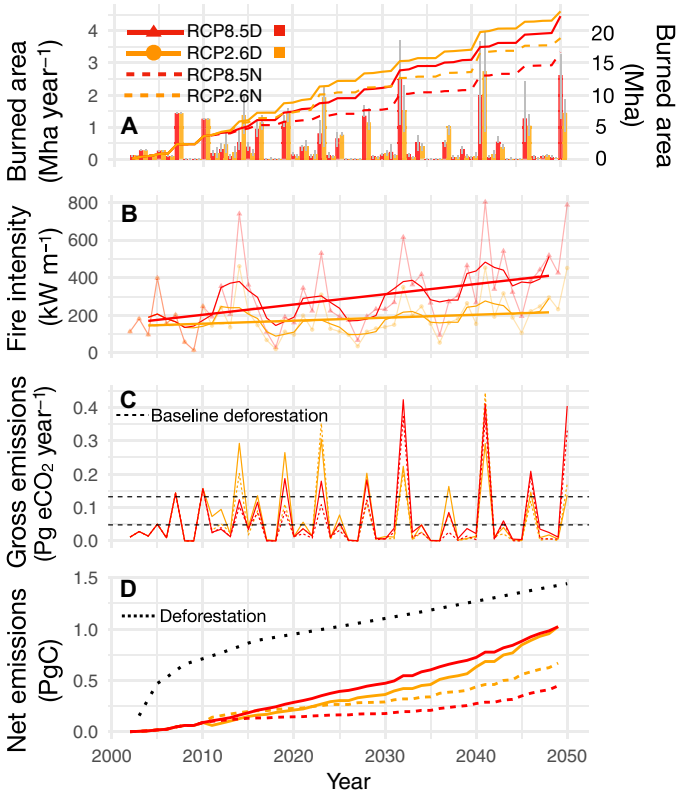

Fig. 4. Fire regime metrics for the southern Brazilian Amazon between 2001 and 2050. (**A**) Annual BA (first *y* axis; bars) and cumulative BA (second *y* axis; lines) projected under two climate change scenarios (RCP2.6 and RCP2.6; solid lines) and two deforestation scenarios (D: BAU; N: no new deforestation; dashed lines). The bars represent only the RCP8.5D and RCP2.6D scenarios. (**B**) Fire intensity, represented by 5-year moving averages (solid lines) and annual values. (**C**) Annual gross C emissions from projected wildfires. Dashed lines represent deforestation-only baselines for the periods 2000–2005 (upper line) and 2006–2010 (lower line). (**D**) Net emissions from modeled deforestation alone (dotted black line) and forest fire scenarios (colored lines).

DISCUSSION

In southern Amazonia, forest fire regimes have drastically changed over the past three decades (*9*–*11*). Interactions between human activities and extreme weather events have triggered wildfires that burn larger areas and emit more C to the atmosphere, even in areas where deforestation has declined (*9*). During the early 21st century, escaped forest fires may have accounted for a third of total emissions from deforestation, with emissions from wildfires likely surpassing those from deforestation in extreme drought years (*9*). Our projections support these previous findings and point to an acceleration of fire activity in southern Amazonia in the coming decades. We show that 16% of the region's forests may burn as the climate becomes drier and hotter in the next few decades. The eCO_2 emissions from these fires could reach 6.0 Pg in the 2050s, compared with 2.1 Pg in the 2000s. If deforestation continues at current (relatively low) levels, emissions from understory forest fires will regularly surpass those from deforestation. Decreasing global GHG emissions to near zero may reduce the likelihood of severe droughts and associated wildfires. However, the projected outcomes of RCP2.6 and RCP8.5 only began to diverge after 2030, suggesting that the region is already committed to substantial warming and drying under both scenarios. This will likely increase wildfire activity in the next decades (*5*, *17*).

Despite the likely intensification of fire regimes in southern Amazonia, avoiding new deforestation could substantially reduce BA and associated emissions. Compared with the (BAU) deforestation scenarios, we project that preventing new Amazon deforestation reduces BA and eCO_2 net emissions by up to 30 and 56% (RCP8.5), respectively. With no deforestation, the perimeter of forests exposed to sources of ignition decreases, leading to lower BA (*18*). However, we observe a nonlinear relationship between forest fragmentation and BA. Across highly fragmented regions, for instance, the lack of forest connectivity limits BA not only because large fragments are unavailable to burn but also because BA is already high at the beginning of our simulations. In contrast, large tracts of primary forest become flammable and experience increased burning, but only when dry-warm climatic conditions drive forest thinning and associated increases in understory dryness, mostly after 2030. Primary forests in southern Amazonia are less likely to burn early in our simulations because of their high canopy cover and associated high fuel moisture, but they become flammable as droughts and high atmospheric VPD increase fuel availability by warming the forest understory and building up fuel loads. There is ample empirical evidence supporting these behaviors in our model, given that soil drying tends to cause increased mortality of large trees and associated fuel availability (*19*–*22*).

As large tracts of primary forest become flammable, our model projects that protected forests will burn more frequently in the coming decades (*12*). Protected forests not only have effectively deterred most deforestation but also promoted high forest fuel continuity due to forest connectivity. Although the moist forest understory inside those areas prevents fires from spreading in most years (*16*), fuel moisture decreases over time in our simulations as droughts became more intense and frequent and the background VPD increases. Consequently, fires in the future will likely burn larger areas inside protected forests, as decreased precipitation, higher temperatures, and understory drying increase the flammability of intact forests. An earlier modeling study with no such dynamic representation (*23*) found that, instead of becoming more flammable over time, a large protected forest in the southern Amazon (Xingu Indigenous Park) could block fire spread in the near future. Regardless, preventing increased BA inside protected areas will require substantial effort to reduce sources of ignition in the face of more intense droughts and increased flammability of protected forests in southern Amazonia. Another important action to constrain wildfires inside protected forests is to constrain human activities that degrade forests, which can cause increases in fuel loads and dryness. Such activities (e.g., logging) occur much more often outside protected areas but could move into those areas in the future if Brazil's enforcement capacity is diminished (*1*).

Droughts controlled most of the spatial-temporal patterns in BA and fire-induced emissions in our simulations, in agreement with recent observations (*11*). Projected regional warming played an important secondary role. Two major assumptions allowed our fire-ecosystem model to represent such patterns. First, drought-induced fuel accumulation and drying in our model changed, as in 2005, when a severe drought caused increased mortality of Amazonian trees (*24*). While this assumption is likely to hold in the near future, modeling drought-induced changes in forest disturbance and fuel dynamics under extreme climate change into the distant future would require explicit representation of physiological processes such as plant hydraulic failure, drought-induced C starvation (*25*), and changes in forest resilience due to CO_2 fertilization (*2*). The development and application of such models for tropical systems have been hampered by our poor understanding of how

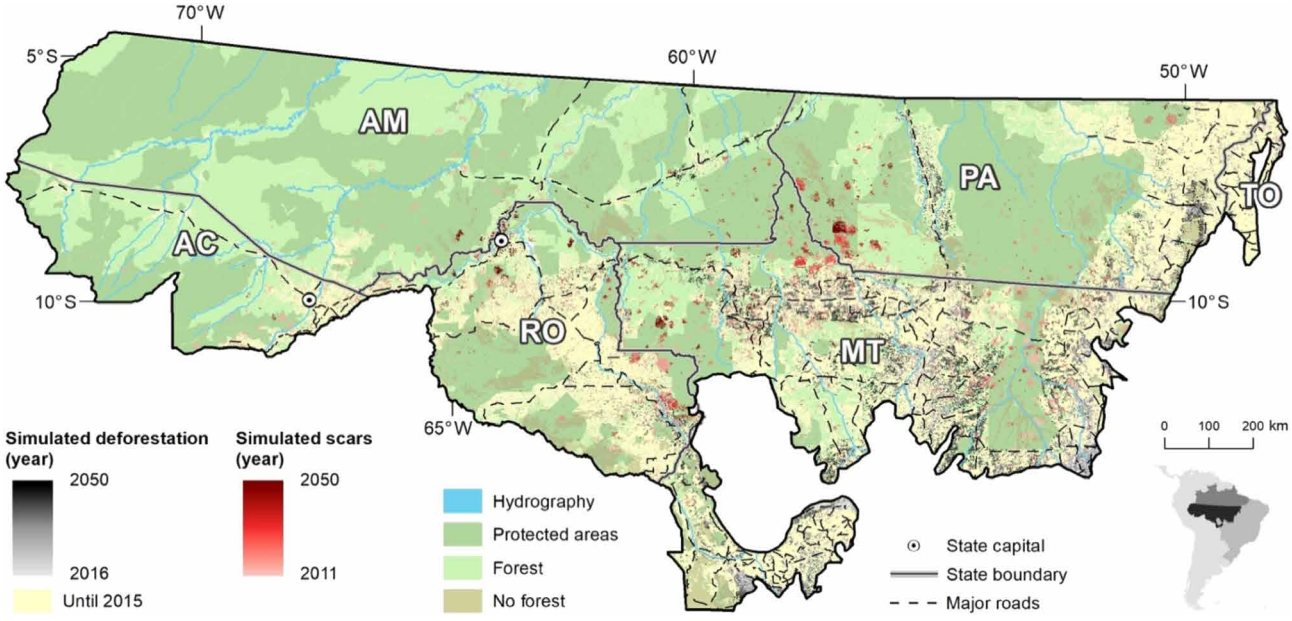

Fig. 5. Projected deforestation and BA. Future projections of fire scars and deforestation for Brazil's southern Amazon from 2011 and 2050 under the RCP8.5D scenario. Darker green represents protected areas and indigenous reserves, while yellow colors show deforested areas.

extended dry periods affect canopy phenology and tree mortality (*26*). Our simulations also lack several stressors that could slow biomass accumulation even further during the recovery period [e.g., liana infestation, nutrient depletion, and windthrow events, among others (*26*)], although our model captured reduced C recovery after fires due to dry-warm climatic conditions, as previously suggested (*27*).

Despite the complex processes affecting fire behavior, intensity, and severity in tropical forests, our modeling approach captured major features of forest fire behavior and severity for southern Amazonia. However, we assume that drought frequency during the 2000s is representative of future drought regimes, while drought intensity and extent will change with future climate projections. This implicitly assumes that the AMO will remain in a warm phase in the coming decades and that drought extent will be similar to that of the 2000s. This characteristic of our model probably underestimated BA and fire-induced C emissions in the central and eastern Amazon, where extended dry periods are also triggered by El Niño–Southern Oscillations (*9*). Advances in climate projections are needed to better represent the teleconnections among future GHG emissions, changes in sea surface temperature anomalies, and Amazon precipitation patterns (*20*). Our model also assumes that all forests in southern Amazonia were equally susceptible to fire, but recent studies point to important variability in bark thickness distribution—the main plant trait controlling fire-induced tree mortality across the basin (*28*, *29*). Had we accounted for such variability, forests in wetter regions would probably exhibit higher fire-induced tree mortality than dry forests, which are more likely to survive wildfires. Last, recurrent fire in our model probably underestimates losses in C stocks after fires, compared with studies in the central Amazon (*20*). Hence, improvements in the model could lead to higher fire-induced C emissions, even with our model simulating slightly higher fire intensity than observed in a large-scale fire experiment (*4*).

The projected intensification of Amazon fire regimes under both RCP2.6 and RCP8.5 climate scenarios in the coming decades underscores the need to counteract increasing fire risk to conserve Amazon forests. Avoiding deforestation could substantially reduce fire-induced GHG emissions (e.g., up to 50% in our simulations), but not enough to offset emission increases associated with climate change. A transition away from fire-dependent to fire-free agriculture and agroforestry systems would reduce sources of ignition and ultimately wildfires (*22*)—a trend that has already been reported in some tropical regions (*30*). Where there is a strong socioeconomic dependence on slash-and-burn systems, fire management techniques should be used to minimize the risk of agricultural fires escaping into neighboring forests while avoiding the negative socioeconomic effects of fire prevention to smallholders and traditional and indigenous peoples (*31*). Command-and-control operations against illegal agricultural fires are another important tool to prevent wildfires (*22*). Furthermore, expanding the existing network of well-trained and equipped fire brigades could enhance Brazil's ability to suppress unwanted fires. Last, specialized weather forecast systems and fire behavior models have effectively guided fire suppression efforts in many countries, often months before the fire season starts (*32*). These strategies could be readily adapted to and implemented in Brazil (*32*).

Aggressive efforts to reduce sources of fire ignition and suppress unwanted fires could reduce the likelihood of burning large tracts of Amazonian forests, including protected areas and indigenous reserves. These actions will be most effective if accompanied by a global decrease in GHG concentrations in the atmosphere. In particular, after 2040, increased GHG emissions may create much more flammable landscapes by triggering widespread droughts and regional warming in Amazonia (*5*). In the absence of sharp reductions in global GHGs to mitigate these negative effects, local and regional efforts to reduce fire probability may yield only short-term results.

MATERIALS AND METHODS

Study area

The study area comprises the meridional Brazilian Amazon, where prolonged dry seasons (3 to 5 months with precipitation ≤100 mm)

create conditions for understory forest fires, especially during drought years. The total modeled area was ~192 Mha, of which 72% is covered by native forests. The main land use in the deforested area was cattle ranching, with mechanized agriculture ranking second (*33*).

Modeling

To address the question of how climate and land use change may affect fire regimes in Amazonia, we used a coupled fire-ecosystem model (*34*, *35*). Our fire model [fire ignition and spread for C (FISC); fig. S1] simulates monthly fire ignition and BA at a resolution of 25 ha for the Amazon region (*34*, *23*), while our ecosystem model [C and land use change (CARLUC)] simulates monthly forest C dynamics as a function of climatic variables (*17*). Both models are implemented using Dinamica EGO modeling platform. Below, we describe each component of the models used in this study.

Fire ignition

FISC estimates the likelihood of agricultural fires igniting a wildfire by combining two probabilities. First is the climatic probability of fire ignition, estimated from monthly maps of climate dryness (e.g., VPD) from the Climate Research Unit (CRU) and National Centers for Environmental Prediction (NCEP)/National Center for Atmospheric Research (NCAR) databases (table S3). Second is the probability of active fires ("hot pixels") occurring in deforested fields near forest edges (≤4 km), estimated annually on the basis of a set of biophysical spatial variables—including location and size of urban areas and deforestation (table S3). Once these probabilities are calculated, FISC evaluates whether their sum exceeds a random number generated according to a beta distribution (*34*). If this random number is exceeded, FISC simulates a successful source ignition (fig. S1) (*1*). This model has been extensively calibrated and validated for the Amazon using active fire data (*23*).

Fire spread

FISC simulates fire propagation using cellular automata. Specifically, if a given forested cell is ignited by an agricultural fire, FISC calculates the probability of this ignition source spreading into each neighboring cell for each model iteration (i.e., 30 per month) (fig. S1). There are four sets of variables defining whether fire spread will occur (table S4): wind intensity and direction (*34*); fine fuel loads estimated by our ecosystem model (CARLUC); terrain features such as upslope direction, obstacles, and different land uses (*34*, *23*); and microclimate conditions (i.e., forest understory VPD) estimated by CARLUC. The fire spread module has been calibrated and validated using fire scar maps from Morton *et al.* (*10*). Our results show that FISC captured the spatial-temporal variability in fire scars across the southern Amazon during the 2000s.

Ecosystem model

CARLUC is a process-based C cycle model that borrows its basic structure from the Physiological Processes Predicting Growth (3 PG) forest model (*35*, *36*). CARLUC estimates net primary productivity from plant available water, photosynthetically active radiation, VPD, and air temperature (table S5). During each monthly time step, net primary productivity is allocated to wood, leaf, and root C pools. Mortality creates necromass that is placed in structural leaf litter, metabolic leaf litter, structural root litter, metabolic root litter, coarse woody debris, and humus pools. Leaf litter and small woody fuels (i.e., 1-hour fuels) are considered as the fuel load (*17*). In addition to C dynamics, CARLUC simulates (i) drought-induced effects on fuel dynamics; (ii) litter moisture content (LMC; %), estimated from VPD; (iii) FSR ($m \cdot min^{-1}$), estimated from LMC; (iv) fire fuel consumption (W; $kg \cdot m^{-1}$), estimated from LMC and fuel load mass; (v) fireline intensity ($kW \cdot m^{-1}$), estimated from FSR and W; and (vi) fire-induced biomass losses, derived from field measurements of fireline intensity (*17*).

CARLUC's representation of the relationship between drought and changes in biomass was derived from the Amazon forest inventory network (*24*). Specifically, changes in aboveground biomass and the ΔMCWD observed during the 2005 drought were compared with the long-term average. CARLUC assumes that when ΔMCWD drops below −40 mm, losses in aboveground biomass occur following a linear function of ΔMCWD (*24*, *37*). This process triggers associated changes in fuel loads and moisture. The fire model has been calibrated for the southern Amazon using data from a large-scale fire experiment (*4*).

Once a given pixel of forest burned, gross GHG emissions occurred in our simulations according to (i) the amount of fuel consumed by the fires (a function of fuel moisture and loads) (*17*); (ii) how much CO_2, CO, CH_4, N_2O, and NO_x our simulated fuel consumption generated, which followed emission factors from the Intergovernmental Panel on Climate Change (*38*); and (iii) how much change in above- and belowground biomass occurred when a given pixel of forest burned. Fire-induced reductions in forest C stocks increased as a function of fire intensity, which is affected by fuel amount and moisture (*17*). In our estimates of gross C emissions, we included eCO_2 derived from fuel combustion and from the decomposition of trees killed by the fires. To calculate net emissions, we assumed that C emissions from tree decomposition were counterbalanced by post-fire vegetation regrowth (as represented by biomass accumulation) over several years. Our model assumed that recovery of C stocks would be total if there were no changes in climatic conditions. In addition, the model assumes that all forests of the Amazon have the same resistance to fire, even when it is affected by fire more than once, which may substantially underestimate fire effects on tree mortality (*17*).

Climate projections

Our fire and ecosystem models were forced with climate data representing two levels of future global radiative forcing, the RCP2.6 and 8.5 W m^{-2}. RCP2.6 assumes negative emissions and is the scenario most closely mirroring the Paris (COP21) agreement. RCP8.5 represents BAU fossil fuel emissions (*39*). To run our fire-ecosystem model, we used simulations from the three climate models participating in the Coupled Model Intercomparison Project Phase 5 (CMIP5) that best represent historical temperature patterns and precipitation seasonality for the Amazon: Hadgem2-es (*40*), Miroc-esm (*41*), and Mri-cgcm3 (*42*) (fig. S2). We used temperature data from the CRU and precipitation from the Tropical Rainfall Measuring Mission (3B42 product) to evaluate and bias-correct these climatic variables.

To estimate potential changes in VPD in the coming decades, we assumed that future changes in air temperature would drive changes in VPD by correcting the mismatch between modeled and observed climate. Specifically, we sliced projected air temperature time series into historical (1950–2005) and future (2006–2050) periods. Next, we estimated the rate of change of temperature (ΔT between historical and future projections). We then modeled the saturation pressure as a function of ΔT (Eq. 1), adding this change in saturation pressure (Δes) to the observed saturation pressure (Eq. 2). Observed saturation pressure and relativity humidity were cycled over the 2000s.

$$\Delta es\,(T) = 0.611 \exp\left(\frac{17.21\Delta T}{\Delta T + 237.3}\right) \quad (1)$$

$$VPD\,(es, rh) = \left(1 - \frac{rhmax}{100}\right)(es + \Delta es) \quad (2)$$

Because the variability in precipitation projected by our climate models was substantially lower than the observed data (*43*), we applied the climate variability from the 2000s to future projections, adding it to the projected changes in precipitation. With this approach, the spatial patterns of drought are constrained mostly to the regions that experienced unusually low precipitation during the 2000s, a decade dominated by drought events associated with the warming phase of the AMO. This prescribed future climate was then used to calculate the MCWD within each decade (*44*).

Deforestation projections

Otimizagro is a spatially explicit model that simulates land use, land use change, forestry, deforestation, and regrowth under various scenarios of agricultural land demand and deforestation policies for Brazil (*45*). The model simulates nine annual crops (including single and double cropping), five perennial crops, and plantation forests. The model framework, developed using the Dinamica EGO platform (*46*), is structured in four spatial levels: (i) Brazil's biomes, (ii) Instituto Brasileiro de Geografia e Estatistica microregions, (iii) Brazilian municipalities, and (iv) a raster grid of 25-ha spatial resolution. Future demand for crops, deforestation, and regrowth rates are exogenous to the model. Projected annual deforestation rates (3100 km^2 $year^{-1}$) (fig. S3) consist of 2009–2014 averages for southern Amazonia [Instituto Nacional de Pesquisas Espaciais (INPE) 2015] (*7*). The spatial distribution of deforestation is a function of spatial determinants, such as distances to roads and previously deforested areas.

Simulations

To simulate potential changes in Amazon fire regimes, we performed four numerical experiments based on future climate and deforestation scenarios. In these experiments, we compared climate and deforestation impacts on fire regimes as a function of two different levels of global warming at the mid-century (2050), the RCP2.6 and RCP8.5 scenarios, and two scenarios of deforestation (no deforestation and deforestation following historical trends).

SUPPLEMENTARY MATERIALS

Supplementary material for this article is available at http://advances.sciencemag.org/cgi/content/full/6/2/eaay1632/DC1

Fig. S1. Components of our modeling framework.
Fig. S2. Spatial-temporal changes in VPD and MCWD for three time periods compared to 2010.
Fig. S3. Projected deforestation for the southern Amazon.
Table S1. Decadal fire-related emissions of different GHG emissions per decade from the 2000s to the 2050s.
Table S2. BA in millions of hectares for each decade and each one of the scenarios representing two deforestation (No deforestation: N; Deforestation: D) and climate pathways (RCP2.6; RCP8.5).
Table S3. Input variables used to run the fire ignition component of our fire model (FISC), the source of the data, and the link to download the data.
Table S4. Input variables used to run the fire spread component of our fire model (FISC), the source of the data, and the link to download the data.
Table S5. Input variables used to run our ecosystem model (CARLUC), the source of the data, and the link to download the data.

REFERENCES AND NOTES

1. C. A. Nobre, G. Sampaio, L. S. Borma, J. C. Castilla-Rubio, J. S. Silva, M. Cardoso, Land-use and climate change risks in the Amazon and the need of a novel sustainable development paradigm. *Proc. Natl. Acad. Sci. U.S.A.* **113**, 10759–10768 (2016).
2. A. Rammig, T. Jupp, K. Thonicke, B. Tietjen, J. Heinke, S. Ostberg, W. Lucht, W. Cramer, P. Cox, Estimating the risk of Amazonian forest dieback. *New Phytol.* **187**, 694–706 (2010).
3. J. K. Balch, P. M. Brando, D. C. Nepstad, M. T. Coe, D. Silvério, T. J. Massad, E. A. Davidson, P. Lefebvre, C. Oliveira-Santos, W. Rocha, R. T. S. Cury, A. Parsons, K. S. Carvalho, The susceptibility of Southeastern Amazon forests to fire: Insights from a large-scale burn experiment. *Bioscience* **65**, 893–905 (2015).
4. P. M. Brando, J. K. Balch, D. C. Nepstad, D. C. Morton, F. E. Putz, M. T. Coe, D. Silvério, M. N. Macedo, E. A. Davidson, C. C. Nóbrega, A. Alencar, B. S. Soares-Filho, Abrupt increases in Amazonian tree mortality due to drought–fire interactions. *Proc. Natl. Acad. Sci. U.S.A.* **111**, 6347–6352 (2014).
5. Y. Le Page, D. Morton, C. Hartin, B. Bond-Lamberty, J. M. C. Pereira, G. Hurtt, G. Asrar, Synergy between land use and climate change increases future fire risk in Amazon forests. *Earth Syst. Dynam.* **8**, 1237–1246 (2017).
6. D. C. Nepstad, C. M. Stickler, B. S. Filho, F. Merry, Interactions among Amazon land use, forests and climate: Prospects for a near-term forest tipping point. *Philos. Trans. R. Soc. Lond. B Biol. Sci.* **363**, 1737–1746 (2008).
7. D. Nepstad, D. McGrath, C. Stickler, A. Alencar, A. Azevedo, B. Swette, T. Bezerra, M. DiGiano, J. Shimada, R. Seroa da Motta, E. Armijo, L. Castello, P. Brando, M. C. Hansen, M. McGrath-Horn, O. Carvalho, L. Hess, Slowing Amazon deforestation through public policy and interventions in beef and soy supply chains. *Science* **344**, 1118–1123 (2014).
8. C. Le Quéré, R. M. Andrew, J. G. Canadell, S. Sitch, J. I. Korsbakken, G. P. Peters, A. C. Manning, T. A. Boden, P. P. Tans, R. A. Houghton, R. F. Keeling, S. Alin, O. D. Andrews, P. Anthoni, L. Barbero, L. Bopp, F. Chevallier, L. P. Chini, P. Ciais, K. Currie, C. Delire, S. C. Doney, P. Friedlingstein, T. Gkritzalis, I. Harris, J. Hauck, V. Haverd, M. Hoppema, K. K. Goldewijk, A. K. Jain, E. Kato, A. Körtzinger, P. Landschützer, N. Lefèvre, A. Lenton, S. Lienert, D. Lombardozzi, J. R. Melton, N. Metzl, F. Millero, P. M. S. Monteiro, D. R. Munro, J. E. M. S. Nabel, S. Nakaoka, K. O'Brien, A. Olsen, A. M. Omar, T. Ono, D. Pierrot, B. Poulter, C. Rödenbeck, J. Salisbury, U. Schuster, J. Schwinger, R. Séférian, I. Skjelvan, B. D. Stocker, A. J. Sutton, T. Takahashi, H. Tian, B. Tilbrook, I. T. van der Laan-Luijkx, G. R. van der Werf, N. Viovy, A. P. Walker, A. J. Wiltshire, S. Zaehle, Global carbon budget 2016. *Earth Syst. Sci. Data* **8**, 605–649 (2016).
9. L. E. O. C. Aragão, L. O. Anderson, M. G. Fonseca, T. M. Rosan, L. B. Vedovato, F. H. Wagner, C. V. J. Silva, C. H. L. Silva Junior, E. Arai, A. P. Aguiar, J. Barlow, E. Berenguer, M. N. Deeter, L. G. Domingues, L. Gatti, M. Gloor, Y. Malhi, J. A. Marengo, J. B. Miller, O. L. Phillips, S. Saatchi, 21st Century drought-related fires counteract the decline of Amazon deforestation carbon emissions. *Nat. Commun.* **9**, 536 (2018).
10. D. C. Morton, Y. Le Page, R. DeFries, G. J. Collatz, G. C. Hurtt, Understorey fire frequency and the fate of burned forests in southern Amazonia. *Philos. Trans. R. Soc. B Biol. Sci.* **368**, 20120163 (2013).
11. A. A. Alencar, P. M. Brando, G. P. Asner, F. E. Putz, Landscape fragmentation, severe drought, and the new Amazon forest fire regime. *Ecol. Appl.* **25**, 1493–1505 (2015).
12. K. Withey, E. Berenguer, A. F. Palmeira, F. D. B. Espírito-Santo, G. D. Lennox, C. V. J. Silva, L. E. O. C. Aragão, J. Ferreira, F. França, Y. Malhi, L. C. Rossi, J. Barlow, Quantifying immediate carbon emissions from El Niño-mediated wildfires in humid tropical forests. *Philos. Trans. R. Soc. B Biol. Sci.* **373**, 20170312 (2018).
13. D. V. Silvério, P. M. Brando, M. M. C. Bustamante, F. E. Putz, D. M. Marra, S. R. Levick, S. E. Trumbore, Fire, fragmentation, and windstorms: A recipe for tropical forest degradation. *J. Ecol.* **44**, 7793–7712 (2018).
14. P. M. Brando, D. Silvério, L. Maracahipes-Santos, C. Oliveira-Santos, S. R. Levick, M. T. Coe, M. Migliavacca, J. K. Balch, M. N. Macedo, D. C. Nepstad, L. Maracahipes, E. Davidson, G. Asner, O. Kolle, S. Trumbore, Prolonged tropical forest degradation due to compounding disturbances: Implications for CO_2 and H_2O fluxes. *Glob. Chang. Biol.* **25**, 2855–2868 (2019).
15. C. V. J. Silva, L. E. O. C. Aragão, J. Barlow, F. Espirito-Santo, P. J. Young, L. O. Anderson, E. Berenguer, I. Brasil, I. Foster Brown, B. Castro, R. Farias, J. Ferreira, F. França, P. M. L. A. Graça, L. Kirsten, A. P. Lopes, C. Salimon, M. A. Scaranello, M. Seixas, F. C. Souza, H. A. M. Xaud, Drought-induced Amazonian wildfires instigate a decadal-scale disruption of forest carbon dynamics. *Philos. Trans. R. Soc. Lond. B Biol. Sci.* **373**, 20180043 (2018).
16. D. Ray, D. Nepstad, P. Moutinho, Micrometeorological and canopy controls of fire susceptibility in a forested Amazon landscape. *Ecol. Appl.* **15**, 1664–1678 (2005).
17. B. L. De Faria, P. M. Brando, M. Macedo, Current and future patterns of fire-induced forest degradation in Amazonia. *Environ. Res. Lett.* **12**, 119601 (2017).
18. A. Alencar, D. Nepstad, M. Carmen Vera Diaz, Forest understory fire in the Brazilian Amazon in ENSO and Non-ENSO years: Area burned and committed carbon emissions. *Earth Interact.* **10**, 1–17 (2006).
19. V. Leitold, D. C. Morton, M. Longo, M. N. Dos-Santos, M. Keller, M. Scaranello, El Niño drought increased canopy turnover in Amazon forests. *New Phytol.* **219**, 959–971 (2018).
20. P. M. Brando, D. C. Nepstad, E. A. Davidson, S. E. Trumbore, D. Ray, P. Camargo, Drought effects on litterfall, wood production and belowground carbon cycling in an Amazon forest: Results of a throughfall reduction experiment. *Philos. Trans. R. Soc. Lond. B Biol. Sci.* **363**, 1839–1848 (2008).

21. P. Meir, P. M. Brando, D. Nepstad, S. Vasconcelos, A. C. L. Costa, E. Davidson, S. Almeida, R. A. Fisher, E. D. Sotta, D. Zarin, G. Cardinot, The effects of drought on Amazonian rain forests. *Geophys. Monogr. Ser.* **186**, 429–449 (2009).
22. D. Nepstad, G. Carvalho, A. C. Barros, A. Alencar, J. P. Capobianco, J. Bishop, P. Moutinho, P. Lefebvre, U. Lopes Silva Jr., E. Prins, Road paving, fire regime feedbacks, and the future of Amazon forests. *For. Ecol. Manage.* **154**, 395–407 (2001).
23. B. Soares-Filho, R. Silvestrini, D. Nepstad, P. Brando, H. Rodrigues, A. Alencar, M. Coe, C. Locks, L. Lima, L. Hissa, C. Stickler, Forest fragmentation, climate change and understory fire regimes on the Amazonian landscapes of the Xingu headwaters. *Landsc. Ecol.* **27**, 585–598 (2012).
24. O. L. Phillips, L. E. Aragão, S. L. Lewis, J. B. Fisher, J. Lloyd, G. López-González, Y. Malhi, A. Monteagudo, J. Peacock, C. A. Quesada, G. van der Heijden, S. Almeida, I. Amaral, L. Arroyo, G. Aymard, T. R. Baker, O. Bánki, L. Blanc, D. Bonal, P. Brando, J. Chave, A. C. de Oliveira, N. D. Cardozo, C. I. Czimczik, T. R. Feldpausch, M. A. Freitas, E. Gloor, N. Higuchi, E. Jiménez, G. Lloyd, P. Meir, C. Mendoza, A. Morel, D. A. Neill, D. Nepstad, S. Patiño, M. C. Peñuela, A. Prieto, F. Ramírez, M. Schwarz, J. Silva, M. Silveira, A. S. Thomas, H. T. Steege, J. Stropp, R. Vásquez, P. Zelazowski, E. Alvarez Dávila, S. Andelman, A. Andrade, K.-J. Chao, T. Erwin, A. Di Fiore, E. Honorio C., H. Keeling, T. J. Killeen, W. F. Laurance, A. Peña Cruz, N. C. Pitman, P. Nuñez Vargas, H. Ramírez-Angulo, A. Rudas, R. Salamão, N. Silva, J. Terborgh, A. Torres-Lezama, Drought sensitivity of the Amazon rainforest. *Science* **323**, 1344–1347 (2009).
25. L. Rowland, A. C. L. da Costa, D. R. Galbraith, R. S. Oliveira, O. J. Binks, A. A. R. Oliveira, A. M. Pullen, C. E. Doughty, D. B. Metcalfe, S. S. Vasconcelos, L. V. Ferreira, Y. Malhi, J. Grace, M. Mencuccini, P. Meir, Death from drought in tropical forests is triggered by hydraulics not carbon starvation. *Nature* **528**, 119–122 (2015).
26. N. McDowell, C. D. Allen, K. Anderson-Teixeira, P. Brando, R. Brienen, J. Chambers, B. Christoffersen, S. Davies, C. Doughty, A. Duque, F. Espirito-Santo, R. Fisher, C. G. Fontes, D. Galbraith, D. Goodsman, C. Grossiord, H. Hartmann, J. Holm, D. J. Johnson, A. R. Kassim, M. Keller, C. Koven, L. Kueppers, T. Kumagai, Y. Malhi, S. M. McMahon, M. Mencuccini, P. Meir, P. Moorcroft, H. C. Muller-Landau, O. L. Phillips, T. Powell, C. A. Sierra, J. Sperry, J. Warren, C. Xu, X. Xu, Drivers and mechanisms of tree mortality in moist tropical forests. *New Phytol.* **219**, 851–869 (2018).
27. C. R. Schwalm, W. R. L. Anderegg, A. M. Michalak, J. B. Fisher, F. Biondi, G. Koch, M. Litvak, K. Ogle, J. D. Shaw, A. Wolf, D. N. Huntzinger, K. Schaefer, R. Cook, Y. Wei, Y. Fang, D. Hayes, M. Huang, A. Jain, H. Tian, Global patterns of drought recovery. *Nature* **548**, 202–205 (2017).
28. P. M. Brando, D. C. Nepstad, J. K. Balch, B. Bolker, M. C. Christman, M. Coe, F. E. Putz, Fire-induced tree mortality in a neotropical forest: The roles of bark traits, tree size, wood density and fire behavior. *Glob. Chang. Biol.* **18**, 630–641 (2012).
29. A. C. Staver, P. M. Brando, J. Barlow, D. C. Morton, C. E. T. Paine, Y. Malhi, A. A. Murakami, J. De Aguila Pasquel, Thinner bark increases sensitivity of wetter Amazonian tropical forests to fire. *Ecol. Lett.* **2019**, 10.1111/ele.13409, (2019).
30. N. Andela, D. C. Morton, L. Giglio, Y. Chen, G. R. van der Werf, P. S. Kasibhatla, R. S. DeFries, G. J. Collatz, S. Hantson, S. Kloster, D. Bachelet, M. Forrest, G. Lasslop, F. Li, S. Mangeon, J. R. Melton, C. Yue, J. T. Randerson, A human-driven decline in global burned area. *Science* **356**, 1356–1362 (2017).
31. T. F. Morello, L. Parry, N. Markusson, J. Barlow, Policy instruments to control Amazon fires: A simulation approach. *Ecol. Econ.* **138**, 199–222 (2017).
32. Y. Chen, J. T. Randerson, D. C. Morton, R. S. DeFries, G. J. Collatz, P. S. Kasibhatla, L. Giglio, Y. Jin, M. E. Marlier, Forecasting fire season severity in South America using sea surface temperature anomalies. *Science* **334**, 787–791 (2011).
33. S. A. Spera, A. S. Cohn, L. K. VanWey, J. F. Mustard, B. F. Rudorff, J. Risso, M. Adami, Recent cropping frequency, expansion, and abandonment in Mato Grosso, Brazil had selective land characteristics. *Environ. Res. Lett.* **9**, 064010 (2014).
34. R. A. Silvestrini, B. S. Soares-Filho, D. Nepstad, M. Coe, H. Rodrigues, R. Assunção, Simulating fire regimes in the Amazon in response to climate change and deforestation. *Ecol. Appl.* **21**, 1573–1590 (2011).
35. A. I. Hirsch, W. S. Little, R. A. Houghton, N. A. Scott, J. D. White, The net carbon flux due to deforestation and forest re-growth in the Brazilian Amazon: Analysis using a process-based model. *Glob. Chang. Biol.* **10**, 908–924 (2004).
36. J. J. Landsberg, R. H. Waring, A generalised model of forest productivity using simplified concepts of radiation-use efficiency, carbon balance and partitioning. *For. Ecol. Manage.* **95**, 209–228 (1997).
37. S. L. Lewis, P. M. Brando, O. L. Phillips, G. M. F. van der Heijden, D. Nepstad, The 2010 Amazon drought. *Science* **331**, 554–554 (2011).
38. IPCC—Intergovernmental Panel on Climate Change 2006 IPCC Guidelines for National Greenhouse Gas Inventories, Prepared by the National Greenhouse Gas Inventories Programme (Kanagawa: Institute for Global Environmental Strategies).
39. D. P. van Vuuren, J. Edmonds, M. Kainuma, K. Riahi, A. Thomson, K. Hibbard, G. C. Hurtt, T. Kram, V. Krey, J.-F. Lamarque, T. Masui, M. Meinshausen, N. Nakicenovic, S. J. Smith, S. K. Rose, The representative concentration pathways: An overview. *Clim. Change* **109**, 5–31 (2011).
40. C. D. Jones, J. K. Hughes, N. Bellouin, S. C. Hardiman, G. S. Jones, J. Knight, S. Liddicoat, F. M. O'Connor, R. J. Andres, C. Bell, K. O. Boo, A. Bozzo, N. Butchart, P. Cadule, K. D. Corbin, M. Doutriaux-Boucher, P. Friedlingstein, J. Gornall, L. Gray, P. R. Halloran, G. Hurtt, W. J. Ingram, J. F. Lamarque, R. M. Law, M. Meinshausen, S. Osprey, E. J. Palin, L. Parsons Chini, T. Raddatz, M. G. Sanderson, A. A. Sellar, A. Schurer, P. Valdes, N. Wood, S. Woodward, M. Yoshioka, M. Zerroukat, The HadGEM2-ES implementation of CMIP5 centennial simulations. *Geosci. Model Dev.* **4**, 543–570 (2011).
41. S. Watanabe, T. Hajima, K. Sudo, T. Nagashima, T. Takemura, H. Okajima, T. Nozawa, H. Kawase, M. Abe, T. Yokohata, T. Ise, H. Sato, E. Kato, K. Takata, S. Emori, M. Kawamiya, MIROC-ESM 2010: Model description and basic results of CMIP5-20c3m experiments. *Geosci. Model Dev.* , 845–872 (2011).
42. S. Yukimoto, Y. Adachi, M. Hosaka, T. Sakami, H. Yoshimura, M. Hirabara, T. Y. Tanaka, E. Shindo, H. Tsujino, M. Deushi, R. Mizuta, S. Yabu, A. Obata, H. Nakano, T. Koshiro, T. Ose, A. Kitoh, A new global climate model of the Meteorological Research Institute: MRI-CGCM3—Model description and basic performance—. *J. Meteorol. Soc. Japan Ser. II* **90A**, 23–64 (2012).
43. P. B. Duffy, P. Brando, G. P. Asner, C. B. Field, Projections of future meteorological drought and wet periods in the Amazon. *Proc. Natl. Acad. Sci. U.S.A.* **112**, 13172–13177 (2015).
44. L. E. O. C. Aragão, Y. Malhi, R. M. Roman-Cuesta, S. Saatchi, L. O. Anderson, Y. E. Shimabukuro, Spatial patterns and fire response of recent Amazonian droughts. *Geophys. Res. Lett.* **34**, L07701 (2007).
45. B. Soares-Filho, R. Rajão, F. Merry, H. Rodrigues, J. Davis, L. Lima, M. Macedo, M. Coe, A. Carneiro, L. Santiago, Brazil's market for trading forest certificates. *PLOS ONE* **11**, e0152311 (2016).
46. B. Soares-Filho, H. Rodrigues, M. Follador, A hybrid analytical-heuristic method for calibrating land-use change models. *Environ. Model. Softw.* **43**, 80–87 (2013).

Acknowledgments: We thank R. Houghton, B. Rogers, P. Duffy, and L. Rattis for helpful suggestions on the manuscript. **Funding:** P.M.B. and B.S.-F. received funding from the World Bank's Program on Forests (PROFOR). B.S.-F. acknowledges support from the project "Development of systems to prevent forest fires and monitor vegetation cover in the Brazilian Cerrado" (World Bank Project no. P143185)–Forest Investment Program (FIP). P.M.B. and M.N.M. were also supported by the NSF (MSB-ECA no. 1802754 and DEB no. 1457602), CNPq (PrevFogo no. 442710/2018-6 and Produtividade no. 310056/2016-0), NASA (IDS no. NNX14AD29G), the Gordon and Betty Moore Foundation (grant nos. 3413 and 5483), and NORAD. D.M. was supported by NASA's Carbon Monitoring System and a Science Without Borders Fellowship from CNPq. **Author contributions:** B.S.-F., L.R., A.A., and P.M.B. designed the model and conducted data analyses. P.M.B. wrote the manuscript with input from all authors. B.S.-F., E.C.M.F., P.M.B., D.M., D.T., M.N.M., U.O., and M.T.C. conceived the study. **Competing interests:** The authors declare that they have no competing interests. **Data and materials availability:** All data needed to evaluate the conclusions in the paper are present in the paper and/or the Supplementary Materials. Model simulation output is archived with the Supplementary Materials, and full datasets may be requested from the authors.

Submitted 24 May 2019
Accepted 8 November 2019
Published 10 January 2020
10.1126/sciadv.aay1632

Citation: P. M. Brando, B. Soares-Filho, L. Rodrigues, A. Assunção, D. Morton, D. Tuchschneider, E. C. M. Fernandes, M. N. Macedo, U. Oliveira, M. T. Coe, The gathering firestorm in southern Amazonia. *Sci. Adv.* **6**, eaay1632 (2020).